European Journal of Medicinal Chemistry 86 (2014) 122–132

Contents lists available at ScienceDirect

European Journal of Medicinal Chemistry

journal homepage: http://www.elsevier.com/locate/ejmech

Original article

Design, synthesis and molecular docking study of novel quinoxalin-2(1*H*)-ones as anti-tumor active agents with inhibition of tyrosine kinase receptor and studying their cyclooxygenase-2 activity

Shadia A. Galal [a, *], Sarah H.M. Khairat [a], Fatma A.F. Ragab [b], Ahmed S. Abdelsamie [a], Mamdouh M. Ali [c], Salwa M. Soliman [d], Jérémie Mortier [d], Gerhard Wolber [d], Hoda I. El Diwani [a]

[a] Department of Chemistry of Natural and Microbial Products, Division of Pharmaceutical and Drug Industries, National Research Centre, Dokki, 12622, Cairo, Egypt
[b] Department of Pharmaceutical Chemistry, Faculty of Pharmacy, Cairo University, Cairo, Egypt
[c] Department of Biochemistry, Division of Genetic Engineering and Biotechnology, National Research Centre, Dokki, 12622, Cairo, Egypt
[d] Department of Pharmaceutical Chemistry, Institute of Pharmacy, Freie University Berlin, Koenigin Luise Strasse, Berlin 14195, Germany

ARTICLE INFO

Article history:
Received 15 March 2014
Received in revised form
9 August 2014
Accepted 14 August 2014
Available online 15 August 2014

Keywords:
Synthesis
Quinoxalines
Antitumor activity
Cyclooxygenase-2
Docking
Protein tyrosine kinase

ABSTRACT

On continuation to our work, new quinoxalin-2(1*H*)-ones were synthesized to study their cytotoxic effect against HepG-2 and MCF-7 with their effect on the human tyrosine kinase (TRK). Compounds **12**, **18**, **15**, **13**, **11a**, **20** and **16**, respectively, were found to be more potent than cisplatin against HepG2 and selective to TRK. Also, compounds **12**, **18**, **20**, **13**, **14**, and **22**, respectively, exhibited decidedly activity against MCF-7 and selectivity against human TRK compared to cisplatin. A molecular docking study was also performed to gain comprehensive understanding into plausible binding modes and to conclude the structure activity relationships of the synthesized compounds. Moreover, anti-inflammatory activity was studied. Compounds **12**, **15**, **18** and **22** were found to be potent and selective against COX-2.

1. Introduction

Quinoxaline derivatives have been identified as a new class of cancer chemotherapeutic agents with significant therapeutic efficacy against solid tumors [1–3]. The two known antineoplastic quinoxaline topoisomerase II poisons are XK469 (NSC697887) and CQS (chloroquinoxaline sulfonamide, NSC339004) (c.f. Fig 1). Compound XK469 (NSC 697887) is a synthetic quinoxaline phenoxy propionic acid derivative that possesses unusual solid tumor selectivity and activity against multidrug resistant cancer cells (Fig 1) [4]. Several lines of evidence indicate that the primary target of XK469 is topoisomerase IIβ. Preferential targeting of topoisomerase IIβ may explain the solid tumor selectivity of XK469 and its analogs because solid tumors, unlike leukemias, often have large populations of cells in the G_1/G_0 phases of the cell cycle in which topoisomerase IIβ is high whereas topoisomerase IIα, the primary target of many selective drugs, is low [5–8]. Chloroquinoxaline sulfonamide is in phase II trial to study the effectiveness in treating patients who have small cell lung cancer that has not responded to platinum-based chemotherapy [9,10].

Protein kinases (PKs) are indispensable for numerous processes in the cell. These enzymes catalyze phosphorylation of different cellular substrates. Phosphorylation in turn regulates various cellular functions. Normally, their activity is stringently regulated. However, under pathological conditions PKs can be deregulated, leading to alterations in the phosphorylation and resulting in uncontrolled cell division, inhibition of apoptosis, and other abnormalities and consequently to diseases [11]. Various cancers and other diseases are known to be caused or accompanied by deregulation of the phosphorylation. Inhibition of PKs has been shown to be a promising therapeutic strategy. A great number of tyrosine kinase inhibitors have been reported [12–14]. The most promising small-molecule selective EGFR-TK inhibitors include quinoxaline e.g. AG 1295 (c.f. Fig 1), a quinoxaline derivative reported to a block

* Corresponding author.
E-mail addresses: sh12galal@hotmail.com, sh12galal@yahoo.com (S.A. Galal).

http://dx.doi.org/10.1016/j.ejmech.2014.08.048
0223-5234/

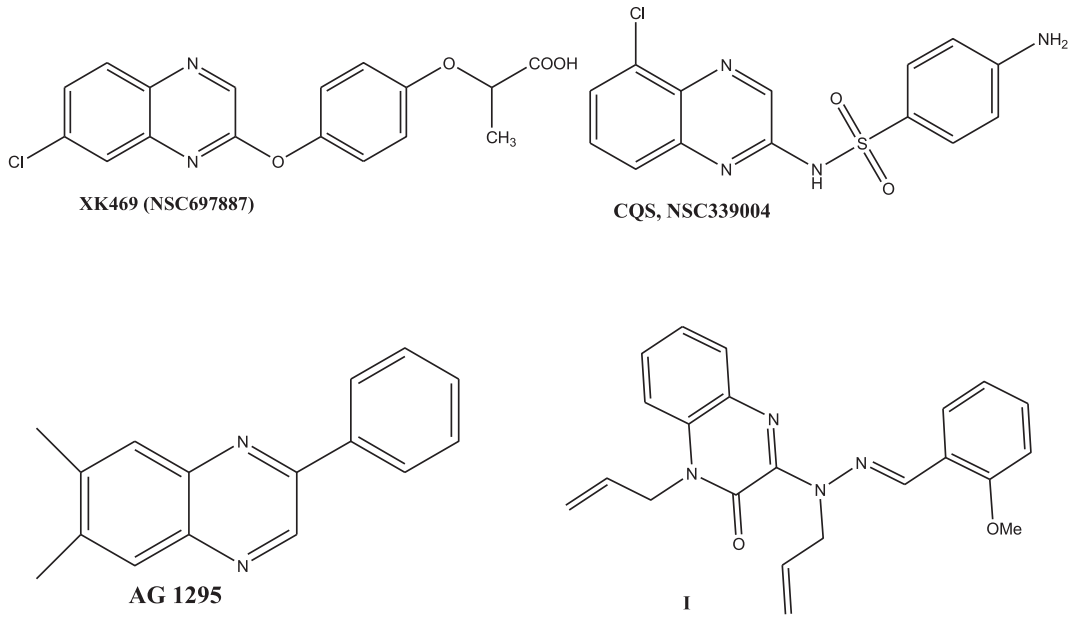

Fig. 1. Structures of potent quinoxalines.

selectively EGFR kinase. This molecule reverses the transformed phenotype of sis-transformed NIH3T3 cells and slow C6 glioma-induced tumors in nude mice [15]. PKs inhibitors (PKIs) have a low molecular weight and most of them bind to protein kinases competing with ATP for the ATP-binding site [16].

The potent cancer chemopreventive activity *in vitro* and in *vivo* of (*E*)-1-allyl-3-(1-allyl-2-(2-methoxybenzylidene)hydrazinyl)quinoxalin-2(1*H*)-one (I) (Fig 1) was discovered by our working group [17]. As a continuation to our research project in preparing antitumor quinoxalines and encouraged by our previous findings, analogs to compound **I** (Fig 1) were synthesized.

The inducible enzyme cyclooxygenase-2 (COX-2) is an important mediator of angiogenesis which plays a role in promoting cancer cell proliferation [18].

The formation of new blood vessels by angiogenesis to provide adequate blood supply is a key requirement for the growth of many tumors. COX-2 is expressed within neovascular structures that support many human cancers. Inhibition of COX-2 delays tumor growth and metastasis [18].

The pyrazole ring is a prominent structural motif found in numerous pharmaceutically active compounds. Pyrazole framework plays an essential role in biologically active compounds and therefore represents an interesting template for combinatorial as well as medicinal chemistry [19–21]. There are many pyrazole derivatives acting as COX-2 inhibitors as celecoxib [22–24], Inhibition of COX-2 by celecoxib delays tumor growth and metastasis [25–29].

The aim of the present investigation was the formation of a new series of quinoxalin-2-one and the introduction of the pyrazole moiety as bioisoster to the aromatic ring of the right-hand side of compound **I**. A series of quinoxaline derivatives was synthesized and tested for the antitumor activity against MCF7 and HepG2 cell lines. Most of the compounds were found to be highly potent and especially compounds **12** and **18** were found to be twice as potent as cisplatin against HepG2 cell line. The new compounds were also tested against human TRK in human liver cancer cell line HepG2 and breast cancer cell line MCF-7. Results showed that most of the tested compounds showed potent inhibition as compared to the inhibition for the untreated cells. Compound **12** inhibited the human TRK activity equal to cisplatin in both cell lines. These results were consistent with cell cytotoxicity activity. Compounds **12**, **15**, **18** and **22** were found to be potent and selective similar to celecoxib against COX-2. The previous data were parallel to the antitumor activity of the tested compounds against HepG2 and MCF-7 cell lines as well as against human TRK inhibition. It can be concluded from the previous findings that the strategy of the present investigation was a very successful one and compounds **12**, **15**, **18**, **11a** and **22** could be lead compounds for further studies in the future.

2. Results and discussion

2.1. Chemistry

A convergent synthesis was designed for the preparation of 3-(pyrazol-4-yl-methylene hydrazinyl) quinoxalin-2(1*H*)-one derivatives **9**–**20**.

The first part of this synthesis involved the preparation of pyrazole derivatives via several steps starting by the synthesis of 3-methyl-1*H*-pyrazol-5-ol derivatives (**1a**,**b**) by reacting ethyl acetoacetate with hydrazines [30] in the presence of glacial acetic acid. Vilsmeier–Haack chloroformylation of the pyrazolones **1a** and **1b** yielded 5-chloro-3-methylpyrazole-4-carboxaldehydes **2a** and **2b** respectively using dimethylformamide and phosphorus oxychloride. Introduction of nucleophiles into 5-chloropyrazole **2a** to produce 5-substituted pyrazoles **3**–**8** was achieved by nucleophilic aromatic substitution with different amines as piperidine, morpholine, piperazine, 1-acetyl-piperazine, 1-benzene sulphonyl piperazine and 1-(2-nitrobenzenesulfonyl)piperazine in the presence of dimethylformamide and sodium hydride (c.f. Scheme 1). Compounds 3-methyl-5-morpholino-1-phenyl-1*H*-pyrazole-4-carbaldehyde (**3**) and 3-methyl-1-phenyl-5-(piperidin-1-yl)-1*H*-pyrazole-4-carbaldehyde (**4**) were synthesized according to reported method of Park et al. [31] The ^{1}H NMR of compounds **5**–**8** showed the appearance of aliphatic signals of the piperazine moiety and the aldehydic CH=O at δ_H 9.8 ppm. The structure of compound **6** was confirmed by the appearance of the acetyl CH_3 signal at δ_H 2.46 ppm and the C=O band at 1604 cm^{-1} in the IR spectrum.

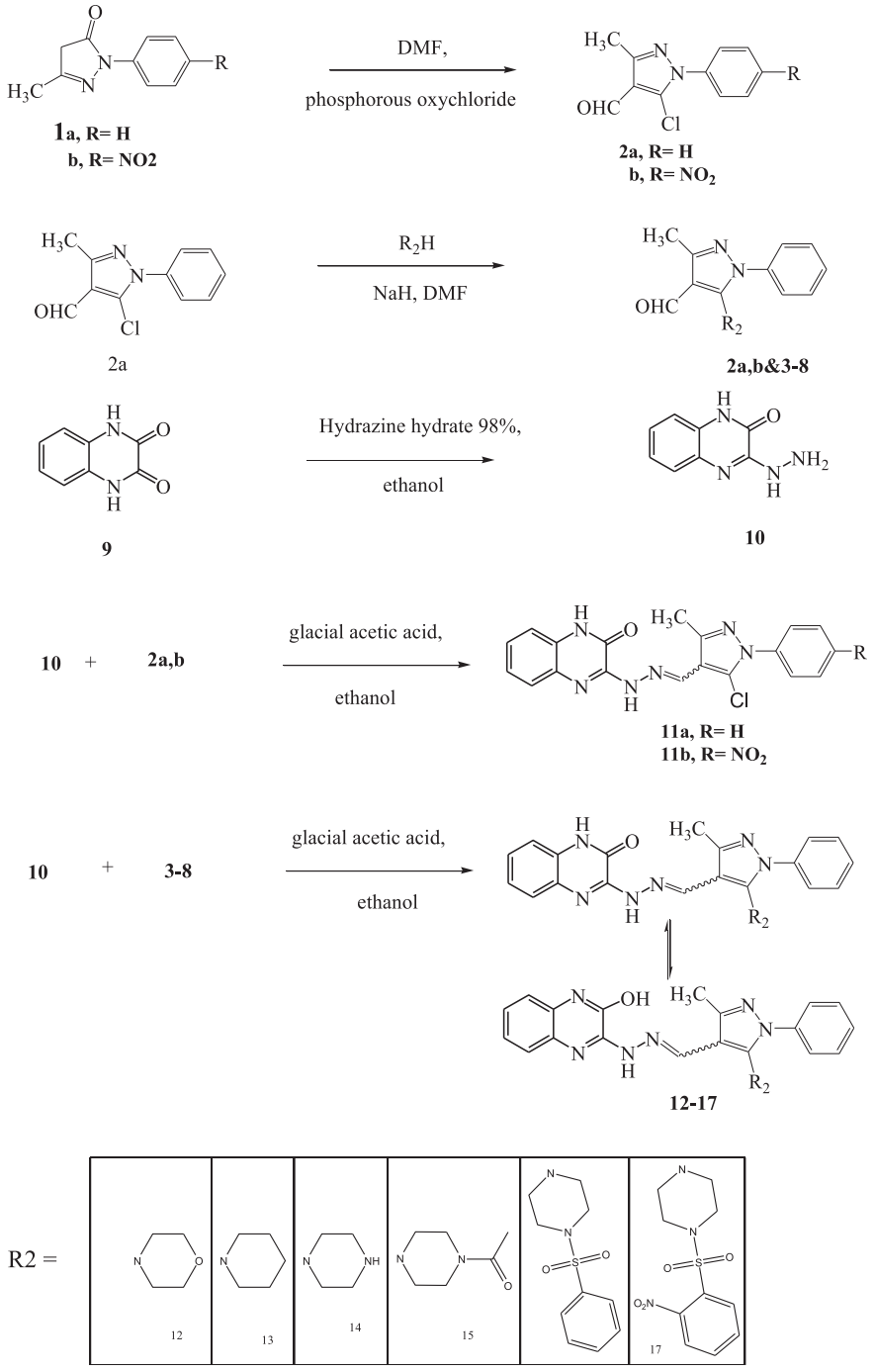

Scheme 1. Synthesis of compounds **2a**,**b** & **3**–**17**.

For compounds **7** and **8**, the presence of extra aromatic protons resonance at δ_H 7.67–7.96 ppm in their ^{1}H NMR spectra proved their structures. The second part of this synthesis started with the preparation 3-hydrazinylquinoxalin-2(1*H*)-one (**10**) that was obtained by reaction of quinoxalin-2,3(*1H,4H*)-dione (**9**) with hydrazine hydrate in ethanol. Compounds **9** & **10** were previously prepared by our laboratory group [17]. Condensation of compounds **2**–**8** with 3-hydrazinylquinoxalin-2(1*H*)-one (**10**) was carried out in the presence of ethanol and glacial acetic acid to obtain the required target compounds **11a**,**b**–**17** (c.f. Scheme 1).

In the last part of this synthesis, dehydrohalogenation took place when compound **11a** reacted with 1-methylpiperazine, cyclopentanol, 2-mercaptoethanol, thioglycolic acid or dimethylamine in the presence of sodium hydride and DMF to form compounds **18**–**22**, respectively (c.f. Scheme 2). The presence of the signals of the aliphatic protons of the introduced moieties in the ^{1}H NMR spectra confirmed the structures of the previous new compounds.

The IR spectra of compounds **11**–**22**, showed the disappearance of aldehydic group of the pyrazole aldehyde that characterized derivatives (**3**–**8**) with the appearance of the quinoxalinyl carbonyl group around 1670 cm^{-1} in the IR spectra. The ^{1}H NMR spectra of compounds proved the condensation between pyrazaldehyde and 3-hydrazinylquinoxalin-2(1*H*)-one (**10**). The presence of the

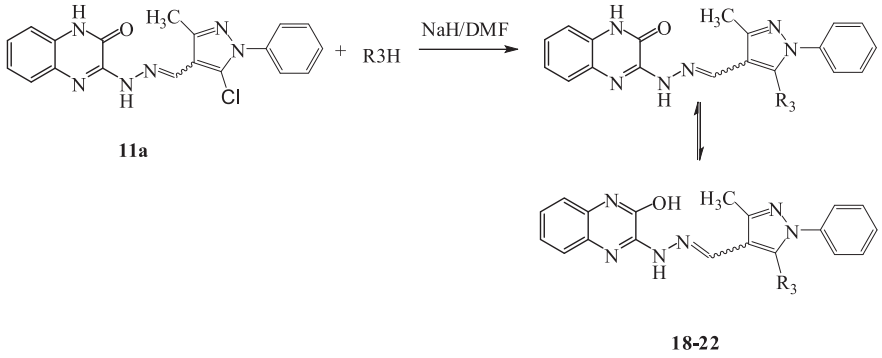

R3 =

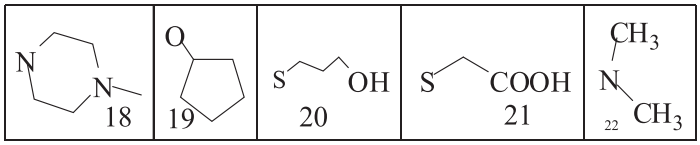

Scheme 2. Synthesis of compounds **18**–**22**.

methine proton (CH═N) signal in the ^{1}H NMR spectra in the range δ_H 8.6–9.04 ppm confirmed the new structures.

Compounds **11**–**22** were present in both keto and enol tautomers. This was confirmed by the ketonic carbonyl band and the intramolecular hydrogen bonded OH band displayed in the IR spectra of the compounds as well as the enolic OH signal D_2O exchangeable as well as the duplication of the aromatic signals in the ^{1}H NMR spectra.

2.2. Cytotoxic activity

Antitumor activity was performed in the National Cancer Institute Cairo University using the method of Skehan et al. [32] The cytotoxic activity of compounds **11a**,**b**–**22** was performed against human liver HepG2 and breast MCF-7 cancer cell lines using cisplatin as reference (c.f. Table 1). All the tested compounds showed remarkable anticancer activity against liver HepG2 cell line. Compounds **12**, **18**, **15**, **13**, **11a**, **20** and **16**, respectively, were found to be more potent than cisplatin. Compounds **22**, **17** and **11b**, respectively, showed less activity than cisplatin. Compounds **19**, **14** and **21** showed moderate antitumor activity. The antitumor activity of the compounds can be arranged in this order compared to cisplatin 12 > **18** > **15** > **13** > **11a** > **20** > **16** > **cisplatin** >**22** > **17** > **11b** > **19** > **14** > **21**. Moreover, all the tested compounds were found to possess high potency against breast MCF-7 cell line. Among the tested compounds, compounds **12**, **18**, **20**, **13**, **17** were more potent than cisplatin, compounds **15**, **22**, **11b** showed potent antitumor activity but less than cisplatin. Whereas the anticancer activity of the compounds compared to cisplatin can be arranged in a decreasing order **12** > **18** > **20** > **13** > **17** > **cisplatin** > **14** > **15** > **22** > **11b** > **11a** > **16** > **19** > **21**.

2.3. Protein kinase inhibition

To study the effect of tested compounds on the level of human tyrosine kinase (TRK), two different human tumor cell lines including breast cancer cell line (MCF-7) and liver cancer cell line (HepG2) were utilized. IC_{50} values of the studied compounds or cisplatin as standard reference drug in DMSO were used. The results showed that most of the tested compounds showed potent inhibition against human TRK in human HepG2 liver and breast MCF-7 cancer cell lines as compared to the inhibition for the untreated cells as listed in (Table 1). In case of HepG2, seven compounds **12**,**18**, **15**, **11a**, **20**, **13** and **22**, respectively, were found to be potent and selective similar to the positive drug, cisplatin (83%) against human TRK with percentage of inhibition values were 84, 83, 80, 79, 78, 75, and 73% respectively as compared with control untreated cells. In case of MCF-7, six compounds **12**, **18**, **20**, **13**, **14**, and **22** were found to be potent and selective similar to the positive drug, cisplatin (84%) against human TRK with percentage of inhibition values were 85, 83, 82, 74, 66, and 62% respectively as compared with control untreated cells. From the foregoing result it is clear that compounds **12** and **18** inhibited the human TRK activity equal to the cisplatin in both cell lines. These results were consistent with cell cytotoxicity activity. Moreover, the human receptor tyrosine kinase (RTK) c-Kit (also referred to as stem cell factor receptor or CD117) is a cytokine receptor expressed on the surface of hematopoietic stem cells as well as other cell types [33]. Altered forms of this receptor may be associated with some types of cancer [33]. C-kit is a receptor tyrosine kinase, which binds to stem cell factor (a substance that causes certain types of cells to grow), known as “steel factor c-kit ligand”. When this receptor binds to

Table 1
The IC_{50} values and the percent of human TRK inhibition of the tested compounds in human liver HepG2 and breast MCF-7 cancer cell lines.

Compounds	IC_{50} (μM)		% of TRK inhibition[a]	
	HepG2	MCF-7	HepG2	MCF-7
11a	19.60 ± 2.10	25.15 ± 2.50	79.00 ± 8.50	34.00 ± 3.60
11b	34.20 ± 3.5	20.71 ± 2.11	39.00 ± 4.37	40.00 ± 4.20
12	11.02 ± 1.12	9.28 ± 0.95	84.00 ± 8.83	85.00 ± 9.00
13	18.06 ± 1.80	12.80 ± 1.32	75.00 ± 7.87	74.00 ± 7.70
14	38.08 ± 3.80	16.31 ± 1.65	20.00 ± 2.40	66.00 ± 7.22
15	11.00 ± 1.30	18.00 ± 1.80	80.00 ± 8.50	–
16	28.12 ± 2.80	26.19 ± 2.63	19.00 ± 2.20	12.00 ± 1.50
17	32.25 ± 3.22	14.30 ± 1.46	13.00 ± 1.55	37.00 ± 4.00
18	11.38 ± 1.20	10.00 ± 1.12	83.00 ± 9.00	83.00 ± 8.90
19	36.45 ± 3.70	31.54 ± 3.20	40.00 ± 5.00	16.50 ± 1.88
20	23.40 ± 2.42	11.26 ± 1.17	78.00 ± 8.10	82.00 ± 8.00
21	40.55 ± 4.16	33.64 ± 3.44	22.00 ± 2.86	4.00 ± 0.60
22	31.52 ± 3.22	18.04 ± 1.83	73.00 ± 7.73	62.00 ± 6.50
DMSO	–	–	–	–
Cisplatin	31.16 ± 3.23	15.71 ± 1.60	83.00 ± 8.75	84.00 ± 8.76

Data were expressed as mean ± S.E. of three independent experiments.
[a] The percentage changes of TRK level as compared with control untreated cells.

stem cell factor it forms a dimer that activates its intrinsic tyrosine kinase activity that in turn phosphorylates and activates signal transduction molecules that propagate the signal in the cell. Signaling through c-kit plays an important role in cell survival, proliferation, and differentiation [33]. So from our results our compounds compete with the tyrosine kinase to the c-kit and prevent activation of the previous pathway resulting in stop cancer cell growth.

2.4. Molecular modeling: docking study

It has been postulated already that the molecular mechanism of quinoxaline derivatives decreasing cell proliferation can be due to inhibition of receptor tyrosine kinase c-kit [17,34]. To investigate their potential mode of action and rationalize the structure activity relationships of this novel series, a molecular docking study was carried out with the c-kit receptor. Using the software LigandScout [35], a 3D pharmacophore was generated from a known inhibitor (Gleevec) co-crystallized in the protein binding site (PDB code 1T46) [36]. The generated structure-based pharmacophore translated the crucial binding features for the inhibition of c-kit and was used to guide the selection of the more plausible binding poses of the newly synthesized compounds. The pharmacophore included two main hydrophobic sub-sites accommodating the hydrophobic moieties of the ligand in the binding pocket. The residues of c-kit found on one side were VAL603, LEU799, PHE811 and THR670, and on the other side ILE653, LEU783, LEU647 and ILE808. Additionally, two key hydrogen bonds with GLU640 and ASP810 stabilizing the inhibitor in the center of the cavity were included into the pharmacophore model. An exclusion volume coat was created to reflect steric constraints by adjacent amino acid in the binding site.

The docking program GOLD was then used to find plausible docking poses for all compounds within the crystal structures of c-kit receptor protein (PDB code: 1T46) [36,37]. The generated docking conformations were ranked based on their ability to meet the above mentioned 3D pharmacophore features. These results are highly correlated to the chemopreventive activity of the compound series.

2.5. Structure–activity relationship

The activity of most of the newly synthesized methylenehydrazinylquinoxalin-2(1*H*)-ones against c-kit may be attributed to the presence of the CH═NN group, which is common in all the compounds and can work as a hydrophilic anchor within a rather hydrophobic binding site. The hydrazone group can stabilize the compounds in the binding pocket through the two key hydrogen bonds involving GLU640 and ASP810, acceptor and donor respectively. The docking study showed compounds deeply embedded into the ATP-binding cleft of c-kit. The docking poses met the pharmacophore features and good complementarities were observed between the docked ligands and the two hydrophobic regions of the cavity. Additionally, other hydrogen bonds observed between the terminal sulfhydryl group of CYS809 and the imidazole ring and between GLU640 and hydroxyl group of quinoxaline hold the compounds tightly in the enzymatic pocket.

For instance, compound **12** (Fig. 2), which displayed one of the highest chemopreventive activity, displays a good complementarily with the pharmacophore described above. First, the typical hydrogen bonds for the catalytic site were identified between GLU640 and ASP810 and the hydrazone group of the ligand, and between the imidazole ring and CYS809, indicating a good overall orientation of the ligand in the cavity. In the first sub-site, the quinoxaline ring is stabilized by residues ILE653, LEU783, LEU647, LEU644 and ILE808, while the phenyl ring interacts with residues VAL603, ALA621 and LEU595 of the second hydrophobic sub-site of the enzyme. Compound **12** shows two extra hydrophobic contacts between the methyl group of the ligand and PHE811, and between the morpholine ring and the same residues that stabilize the phenyl ring (ALA621 and VAL603). Moreover, the morpholine group makes a hydrogen bond with THR670, which can explain its improved activity over other compounds.

Generally, the hydrophobic substitution on the imidazole ring improves the anti-proliferation effect of our compounds. This can be rationalized by the good ligand-protein complementarities in this region of the c-kit cavity. This can be observed with compounds **11a** and **11b**, substituted in this position with chlorine and having a high activity, but less than compound 7. Moreover, substituting the chlorine atom with larger six-member heterocyclic moieties increased the activity of compounds **12**, **18**, **15** against HepG-2 and MCF-7. As mentioned previously, the morpholine derivative (in compound **12**) capable of both hydrophobic contact and hydrogen accepting interaction displayed higher activity than the piperidine derivative (in compound **13**), that makes only hydrophobic contact. The piperazine substitution (in compound **14**) reduces the potential hydrophobic contact and is not capable of accepting a hydrogen bond, which can explain the lowest measured activity among the six-member heterocyclic rings. Interestingly, substituting the NH of piperazine by a methyl that induces potential extra hydrophobic contact (compound **18**) or an acetyl group capable of a hydrogen bond with THR670 (compound **15**) correlates with the increased activity of these two molecules over compound **14**. Furthermore, no favored interaction in the binding cavity could be observed with the five-member ring displayed, explaining the limited activity of compound **19**. Likewise, adding flexible substitutions on the imidazole ring has a negative effect on the activity, as observed with compound **20**. Compound **21** displayed the low cancer activity. This can be explained by the polar carboxylate group linked to the imidazole ring, which is inadequate for binding the c-kit subpocket.

As retrieved from cell line data, addition of an electron withdrawing group on the phenyl group either directly attached to pyrazol ring or to piperazine phenyl sulfonyl group increases the selectivity towards MCF-7 cell line. As a result, NO_2 on the phenyl ring in **11b** decreases the activity against HepG-2 than **11a** but more favored for MCF-7. Likewise, compound **16** has less activity against HepG-2 and more against MCF-7 in comparison with compound **17**.

2.6. In vitro cyclooxygenase inhibition assay

COX expression has been found to be up regulated in most human tumors including colon, lung, breast and prostate, which also attributes to cancer-related inflammation, tumor cell proliferation, resistance to apoptosis and angiogenesis [38]. So we study the ability of the tested compounds to inhibit ovine COX-1 and COX-2 using an enzyme immunoassay (EIA) kit. The efficacies of the tested compounds were determined as the concentration causing 50% enzyme inhibition (IC_{50}) (Table 2). All the tested compounds showed no inhibition of COX-1 up to 50 μM. Moreover, a reasonable *in vitro* COX-2 inhibitory activity was observed with compounds **12**, **15**, **18** and **22** with IC_{50} 0.50, 0.46, 0.48, 0.4, μM respectively. The selectivity indices (COX-1/COX-2) were calculated and compared with that of the standard COX-2 selective inhibitor, celecoxib.

In the assay system, the IC_{50} values of celecoxib on COX-1 and COX-2 were determined to be > 50 and 0.28 μM, indicating that celecoxib is a selective COX-2 inhibitor. The results showed that most of the compounds showed potent inhibition against COX-2 (IC_{50}: 0.40–8.50 μM) compared to the inhibition for COX-1 (IC_{50} > 50 μM) as listed in (Table 2). Four of the compounds (**12**,

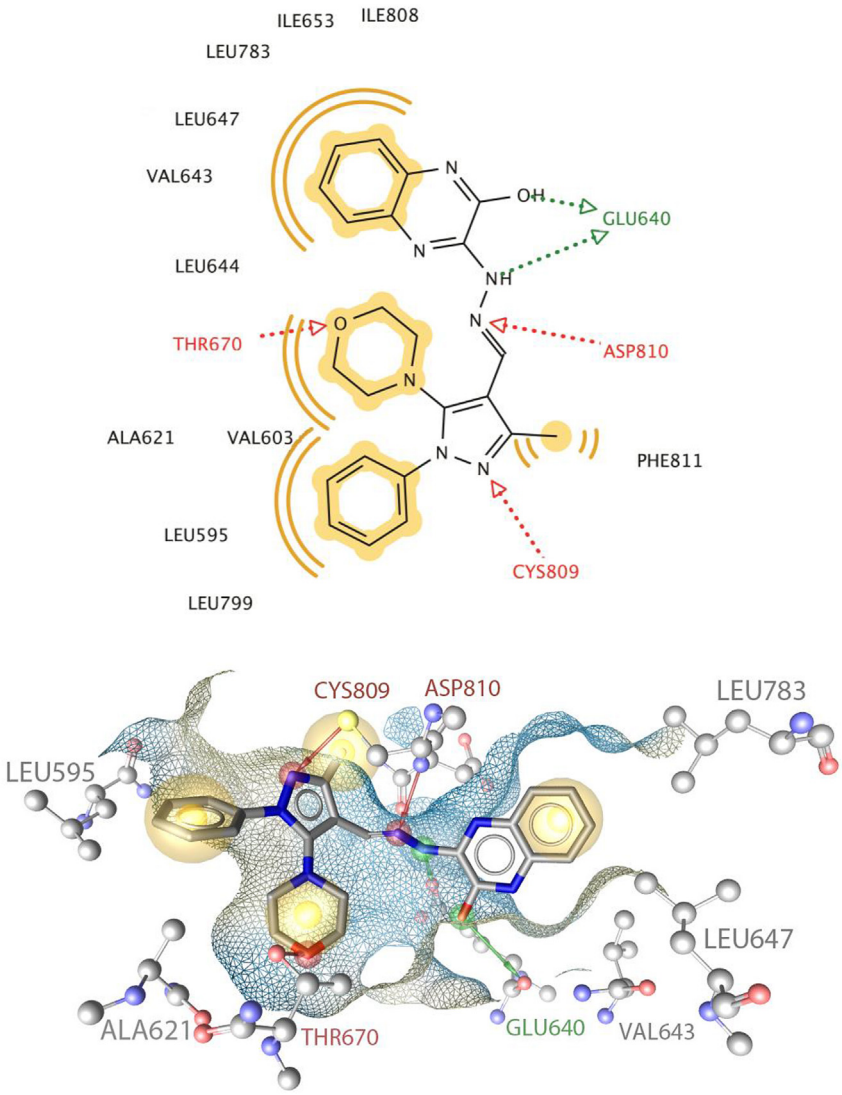

Fig. 2. Proposed binding mode for compound **12** in 2D (up) and 3D (down) showing favorable hydrophobic contacts (yellow spheres) and four hydrogen bonds with GLU640 (green), ASP810 (red), THR670 (red), and CYS809 (red). To insure clarity, not all interacting amino acids are shown in 3D presentation. (For interpretation of the references to color in this figure legend, the reader is referred to the web version of this article.)

15, **18** and **22**) were found to be potent and selective similar to celecoxib against COX-2. The previous data were parallel to the antitumor activity of the tested compounds against HepG2 and MCF-7 cell lines as well as against human TRK inhibition.

Table 2
Data of the *in vitro* COX-1/COX-2 enzyme inhibition assay of the designed compounds.

Compound no.	IC_{50} (μM)[a]		SI[b]
	Cox-1	Cox-2	
11a	>50	32.00 ± 3.90	1.60 ± 0.19
12	>50	0.50 ± 0.06	100.00 ± 11.72
13	>50	22.00 ± 3.10	2.30 ± 0.27
14	>50	16.00 ± 1.87	3.12 ± 0.34
15	>50	0.46 ± 0.05	108.70 ± 12.77
18	>50	0.48 ± 0.06	104.20 ± 11.00
19	>50	8.50 ± 0.97	5.90 ± 0.66
22	>50	0.40 ± 0.04	125.00 ± 13.18
Celecoxib	>50	0.28 ± 0.03	178.60 ± 19.20

[a] IC_{50} value is the compound concentration required to produce 50% inhibition of COX-1 or COX-2. Data were expressed as mean ± S.E. of three independent experiments.
[b] Selectivity index (SI) (COX-1 IC_{50}/COX-2 IC_{50}).

3. Conclusion

Studying the antitumor activity of the new compounds against HepG2 and MCF-7 cancer cell lines, it was that most of the compounds were found to be potent and especially compounds **12** and **18** possess high potency against breast cell line and were more potent than cisplatin. Also, compounds **12** and **18** were twice as potent as cisplatin against HepG2 cell line. Compounds **11a**, **13**, **15** were more potent than cisplatin. The results showed that most of the tested compounds exhibited potent inhibition against human TRK in human liver cancer cell line HepG2 and breast cancer cell line MCF-7 as compared to the inhibition for the untreated cells. Compound **12** inhibited the human TRK activity equal to cisplatin in both cell lines. Molecular modeling study revealed the importance of the hydrazone group – common in all synthesized compounds – in stabilizing the docked inhibitors in the hydrophobic binding cleft with 2 H-bonds with GLU640 and ASP810. Moreover, the hydrogen accepting bond between CYS809 and the imidazole ring of high importance for good orientation in the binding pocket. Additionally, this study revealed that lipophilic substitution on the imidazole ring shows good ligand-protein complementarities in this

region of the c-kit cavity, which consequently affects their inhibition potency. These results were consistent with cell cytotoxicity activity. The previous data were parallel to the antitumor activity of the tested compounds against HepG2 and MCF-7 cell lines as well as against human TRK inhibition. It can be concluded from the previous findings that the strategy of the present investigation was a very successful one and compounds **12**, **15**, **18**, **11a** and **22** could be lead compounds for further studies in the future. Four compounds **12**, **15**, **18** and **22** were found to be potent and selective similar to celecoxib against COX-2.

4. Experimental

Microanalyses, spectral data of the compounds were performed in the Micro analytical National Research Centre, Cairo, Egypt. The IR spectra (4000–400 cm^{-1}) were recorded using KBr pellets in a Jasco FT/IR 300E Fourier transform infrared spectrophotometer on a Perkin Elmer FT-IR 1650 (spectrophotometer). The ^1H and ^{13}C NMR spectra were recorded using Joel EX-270 MHz and 500 MHz NMR spectrophotometers. Chemical shifts are reported in parts per million (ppm) from the tetramethyl silane resonance in the indicated solvent. Coupling constants are reported in Hertz (Hz); spectral splitting partners are designed as follow: singlet (s); doublet (d); triplet (t); multiplet (m). Column chromatography was performed on Merck silica gel 60 (200–400 mesh). The mass spectra were carried out using Finnigan mat SSQ 7000 (Thermo. Inst. Sys. Inc., USA) spectroscopy at 70 eV.

4.1. Preparation of compounds *5*–*8*

4.1.1. General procedure

A solution of compound **2a** (5.6 mmol) dissolved in absolute DMF was added drop wise to a solution of piperazine, 1-acetylpiperazine,1-benzenesulfonylpiperazine or 1-(2-nitrobenzenesulfonyl) piperazine (5.6 mmol) dissolved in DMF and NaH. The reaction was refluxed for 18–24 h. Completion of the reaction is monitored by TLC, and then it was poured on crushed ice and the formed solid was filtered off and purified on silica gel column using Ethyl acetate: Petroleum ether: ethanol (5:1.5:1).

4.1.2. 3-Methyl-1-phenyl-5-(piperazin-1-yl)-1H-pyrazole-4-carbaldehyde (*5*)

R_f: 0.52 (Ethyl acetate: Petroleum ether (1.5:1)), yield: 65%, m.p.: 170–173. IR (KBr, υ_{max}/cm^{-1}) 3431 (NH of piperazine), 2920 (CH aliphatic), 1664 (CHO). ^1H NMR (DMSO-d_6, 500 MHz), 2.37 (s, 3H, CH_3 of pyrazole), 3.04–3.08 (m, 4H, H3, H5 of piperazine moiety), 3.37 (m, 4H, H2, H6 of piperazine moiety), 7.42–7.51 (m, 5H, H2, H3, H4, H5 of phenyl moiety), 9.07 (s, 1H, NH, D_2O exchangeable), 9.8 (s, 1H, CHO) MS: [*m*/*z*(rel. abundance)]: 270 (M^+, 15.8%), 271 (M^++1, 4.46%), 186 (20.4%). Anal. Calcd for $C_{15}H_{18}N_4O$ (FW: 270): C, 66.64; H, 6.71; N, 20.73. Found: C, 65.59; H, 5.78; N, 20.68.

4.1.3. 5-(4-Acetylpiperazin-1-yl)-3-methyl-1-phenyl-1H-pyrazole-4-carbaldehyde (*6*)

R_f: 0.5 (Ethyl acetate: Petroleum ether (2:1)), yield: 70%, m.p.: 123–127 °C. IR (KBr, υ_{max}/cm^{-1}): 3114 (CH aromatic), 2920 (CH aliphatic), 1674 (CHO), 1654 (C=O). ^1H NMR (DMSO-d_6, 500 MHz), 2.3 (s, 3H, CH_3 of pyrazole moiety), 2.46 (s,3H, CH_3 acetyl), 3.0–3.03 (m, 4H, H2, H6, of piperazine moiety), 3.31–3.33 (m, 4H, H3, H5, of piperazine moiety), 7.42–7.52 (m, 5H, H2, H3, H4, H5 of phenyl moiety), 9.88 (s, 1H, CHO group) moiety). MS: [*m*/*z*(rel. abundance)]: 312 (M^+, 44.26%), 299 (28.69%), 69 (100%). Anal. Calcd for $C_{17}H_{20}N_4O_2$ (FW: 312): C, 65.37; H, 6.45; N, 17.94. Found: C, 65.42; H, 6.00; N, 17.84.

4.1.4. 5-(4-(-Benzenesulfonyl) piperazin-1-yl) 3-methyl-1-phenyl-1H-pyrazole-4-carbaldehyde (*7*)

R_f: 0.44 (ethyl acetate: Petroleum ether (1.5:1)), yield: 60%, m.p.: 145–149. IR (KBr, υ_{max}/cm^{-1}): 3068 (CH aromatic), 2921 (CH aliphatic), 1665 (CHO of pyrazole). ^1H NMR (DMSO-d_6, 500 MHz), 2.3 (s, 3H, CH_3), 3.01–3.07 (m, 4H, H2, H6 of piperazine moiety), 3.45–3.50 (m, 4H, H3, H5 of piperazine moiety), 7.32–7.36 (m, 3H, H3, H4, H5 of phenyl moiety),7.4–7.57 (m, 5H, H2, H6 of phenyl moiety, H3, H4, H5 of benzenesulfonyl moiety), 7.67–7.9 (m, 2H, H2, H6 of benzenesulfonyl moiety), 9.8 (s, CHO group). MS: [*m*/*z* (rel. abundance)]: 410 (M^+, 18.25%), 412 (M^++2, 2.47%), 225 (100%). Anal. Calcd for $C_{21}H_{22}N_4O_3S$ (FW: 410): C, 61.44; H, 5.40; N, 13.65; S, 7.81. Found: C, 61.49; H, 5.30; N, 13.72; S, 7.78.

4.1.5. 5-(4-(2-Nitrobenzenesulfonyl)piperazin-1-yl)-3-methyl-1-phenyl-1H-pyrazole-4-carbaldehyde (*8*)

R_f: 0.58 (ethyl acetate: petroleum ether: ethanol (2:1: 0.25)), yield: 60%, m.p.: 198–201 °C. IR (KBr, υ_{max}/cm^{-1}) 3070 (CH aromatic), 2914 (CH aliphatic), 1665 (CHO group), 1544 & 1355, (NO_2), 1455& 1268 (SO_2). ^1H NMR (DMSO-d_6, 500 MHz), 2.39 (s, 3H, CH_3), 3.36–3.39 (m, 4H, H3, H5 of piperazine moiety), 3.71–3.78 (m, 4H, H2, H6 of piperazine moiety), 7.4–7.47 (m, 5H, H2, H3, H4, H5, H6 of phenyl moiety), 7.5 (m,1H, H4 of nitrobenzenesulfonyl), 7.95–7.96 (m, 3H, H3, H5, H6 of nitrobenzenesulfonyl group), 9.89 (s, 1H, CHO group). MS: [*m*/*z* (rel. abundance)]: 455 (M^++1, 49.21%). Anal. Calc for $C_{21}H_{21}N_5O_5S$ (FW: 455): C, 55.37; H, 4.65; N, 15.38; S, 7.04. Found: C, 55.51; H, 3.99; N, 15.44; S, 6.14.

4.1.6. General procedure for the preparation of compounds *11a,b*–*17*

A solution of compound **2a**, **2b** or **3**–**8** (5.6 mmol) in absolute ethanol (15 mL) was added to a solution of 3-hydrazinylquinoxalin-2(1*H*)-one (**10**) (5.6 mmol) in absolute ethanol (15 mL) and glacial acetic acid (2 mL) was added. The reaction mixture was refluxed for appropriate time 5–12 h. Completion of the reaction was monitored by TLC, and then it was cooled and poured on crushed ice and neutralized by ammonia solution. The formed solid was filtered off and crystallized from ethanol.

4.1.7. 3-(2-((5-Chloro-3-methyl-1-phenyl-1H-pyrazol-4-yl) methylene)hydrazinyl)quinoxalin-2(1H)-one (*11a*)

R_f: 0.64 (ethyl acetate: petroleum ether, 1.5: 1) yield: 95%, m.p.: 242–245 °C. IR (KBr, υ_{max}/cm^{-1}) 3431 (NH quinoxaline), 3352 (NH hydrazinyl), 3042 (CH aromatic), 3000 (intramolecular hydrogen bonded OH), 2995, 2920 (CH aliphatic), 1689 (C=O carbonyl), 1638, 1624 (C=N), 1587 (C=C aromatic). ^1H NMR (DMSO-d_6, 500 MHz), 2.46 (s, 3H, CH_3), 7.16–7.21 (m, 3H, H3, H4, H5 of phenyl protons), 7.40–7.47 (m, 2H, H2, H6 of phenyl protons), 7.53–7.56 (m, 4H, quinoxaline protons), 8.56 (s, IH, CH=N), 11.18 (s, 1H, NH, D_2O exchangeable), 12.32 (s, 1H, NH, D_2O exchangeable).^{13}C NMR (DMSO-d_6, 100 MHz): 14.87, 114.31, 115.46, 123.9, 124.98, 125.37, 126.06, 127.04, 129.05, 129.14, 129.76, 133.37, 137.83, 139.17, 146.54, 148.84, 151.3, 172.5 [*m*/*z* (rel. abundance)]: 378 (M^+, 16%), 380 (M^++2, 3%), 341 (12%), 218 (10%), 160 (100). Anal. Calcd for $C_{19}H_{15}ClN_6O$ (FW: 378.10): C, 60.24; H, 3.99; Cl, 9.36; N, 22.19. Found: C, 60.41; H, 3.78; Cl, 9.44; N, 22.11.

4.1.8. 3-(2-((5-Chloro-3-methyl-1-(4-nitrophenyl)-1H-pyrazol-4-yl)methylene)hydrazinyl)quinoxalin-2(1H)-one (*11b*)

R_f: 0.25 (ethyl acetate/petroleum ether, 3:0.5), yield: 56%, m.p.:285–288 °C. IR (KBr, υ_{max}/cm^{-1}) 3383 (NH quinoxaline), 3316 (NH hydrazinyl), 3033 (CH aromatic), 2849 (CH aliphatic), 1674 (C=O carbonyl), 1613 (C=N), 1572 (C=C aromatic), 1546, (NO_2), 1436 (NO_2). ^1H NMR (DMSO-d_6, 500 MHz), 2.95 (s, 3H, CH_3), 7.086–7.38 (m, 2H, H2, H6, of phenyl protons), 7.38–7.43 (m, 2H, quinoxaline

protons), 8.01–8.12 (m, 2H, quinoxaline protons), 8.22–8.35 (m, 2H, H3, H5 of phenyl protons), 8.55 (s, 1H, CH=N), 9.69 (s, 1H, NH, D_2O exchangeable), 11.98 (s, NH, D_2O exchangeable). ^{13}C NMR (DMSO-d_6, 125 MHz): 14.19, 113.9, 115.32, 116.65, 117.34, 118.98, 121.74, 123.14, 123.51, 125.28, 125.54, 129.98, 133.85, 144.54, 149.64, 152.48, 155.41, 162.91. MS: [*m*/*z* (rel. abundance)]: 423 (M^+, 16%), 425 (M^++2, 3%), 105 (100%). Anal. Calcd for $C_{19}H_{14}ClN_7O_3$ (FW: 423.08): C, 53.85; H, 3.33; Cl, 8.37; N, 23.13. Found: C, 53.78; H, 3.46; Cl, 8.50; N, 23.33.

4.1.9. 3-(2-((3-Methyl-5-morpholino-1-phenyl-1H-pyrazol-4-yl) methylene)hydrazinyl)quinoxalin-2(1H)-one (**12**)

R_f: 0.44 (ethyl acetate: petroleum ether) (1.5:1) yield = 65%, m.p.: 235–236 °C. IR (KBr) (υ_{max}/cm^{-1}) 3422 (NH quinoxaline), 3247 (NH hydrazinyl), 3000 (Intramolecular hydrogen bonded NH), 3056 (CH aromatic), 2962, 2914 (CH aliphatic), 1693 (C=O quinoxaline), 1629, 1606 (C=N). ^1H NMR (DMSO-d_6, 500 MH_Z): ^1H NMR (DMSO-d_6, 500 MH_Z): 2.40 (s, 3H, CH_3), 2.95–3.07 (m, 4H, H2, H6 of morpholine protons), 3.5–3.65 (m, 4H, H3, H5 of morpholine protons), 7.1–7.2 (m, 3H, H3, H4, H5 of phenyl protons), 7.3–7.4 (m, 2H, H2, H6 of phenyl protons), 7.47–7.5 (m, 2H, quinoxaline protons), 7.52–7.6 (m, 2H, quinoxaline protons), 8.7 (s, 1H, CH=N), 11.06 (s, NH, D_2O exchangeable), 11.06 (s, NH, D_2O exchangeable).

^{13}C NMR (DMSO-d_6, 125 MHz): ^{13}C NMR (DMSO-d_6, 125 MHz): 15.07, 21.60, 23.94, 26.21, 51.659, 109.46, 115.49, 123.08, 124.44, 127.41, 129.04, 129.20, 139.75, 141.5, 148.18, 150.41, 151.50, 172.59. MS: [*m*/*z* (rel. abundance)]: 430 (M^++1, 4.91%), 429 (M^+, 3.35%), 387 (10%), 254 (100%), 161 (42.7%), 239 (9.49%). Anal. Calcd for $C_{23}H_{23}N_7O_2$ (FW: 429.19): C, 64.32; H, 5.40; N, 22.83. Found: C, 64.09; H, 5.33; N, 22.98.

4.1.10. 3-(2-((3-methyl-1-phenyl-5-(piperidin-1-yl)-1H-pyrazol-4-yl)methylene)hydrazinyl)quinoxalin-2(1H)-one (**13**)

R_f: 0.52 (Ethyl acetate: petroleum ether, (1.5:1)), yield: 65%, m.p.: 256–259 °C. IR(KBr) (υ_{max}/cm^{-1}) 3441, 3306 (NH of quinoxaline), 3217 (NH hydrazinyl), 3051 (CH aromatic), 2938 (CH aliphatic), 1682 (C=O quinoxaline), 1610 (C=N), 1532 (C=C aromatic). ^1H NMR (DMSO-d_6, 500 MHz): 1.45–1.49 (m, 6H, H3, H4, H5 of piperidine protons), 2.39 (s, 3H, CH_3), 2.99–3.04 (m, 4H, H2, H6 of piperidine protons), 7.1–7.2 (m, 3H, H3, H4, H5 of phenyl protons), 7.3–7.39 (m, 2H, H2, H6 of phenyl protons), 7.44–7.5 (m, 2H, quinoxaline protons), 7.58–7.62 (m, 2H, quinoxaline protons), 8.73 (s, 1H, CH=N), 11.04 (s, NH, D_2O exchangeable), 12.28 (s, NH, D_2O exchangeable). ^{13}C NMR (DMSO-d_6, 125 MHz): 14.9, 21.5, 50.8, 66.99, 109.42, 115.47, 123.90, 124.61, 124.89, 125.90, 127.7, 129.04, 129.32, 133.78, 139.59, 141.20, 146.61, 148.24, 151.49, 172.58.

MS: [*m*/*z* (rel. abundance)]: 428 (M^+ +1, 34%), 268 (95%), 252 (100%), 161 (39%). Anal. Calcd for ($C_{24}H_{25}N_7O$ FW: 427): C, 67.43; H, 5.89; N, 22.93. Found: C, 67.61; H, 5.69; N, 22.78.

4.1.11. 3-(2-((3-methyl-1-phenyl-5-(piperazin-1-yl)-1H-pyrazol-4-yl)methylene)hydrazinyl)quinoxalin-2(1H)-one (**14**)

R_f: 0.2 (Petroleum ether/Ethyl acetate, (0.5: 3)) yield = 65%, m.p: 259–261 °C. IR (KBr) (υ_{max}/cm^{-1}) 3423 (NH of quinoxaline), 3220 (NH hydrazinyl), 3057 (CH aromatic), 3000 (Intramolecular hydrogen bonded NH), 2923, 2856 (CH aliphatic), 1678 (C=O of quinoxaline), 1617 (C=N), 1499 (C=C aromatic). ^1H NMR (DMSO-d_6, 500 MHz): ^1H NMR (DMSO-d_6, 500 MHz): 2.41 (s, 3H, CH_3), 3.08–3.14 (m, 4H, H2, H6 of piperazine protons), 3.14–3.33 (m, 4H, H3, H5 of piperazine protons), 7.04–7.13 (m, 3H, H3, H4, H5 of phenyl protons), 7.27–7.35 (m, 2H, H2, H6 of phenyl protons), 7.39–7.42 (m, 2H, quinoxaline protons), 7.59–7.63 (m, 2H, quinoxaline protons), 8.74 (s, 1H, CH=N), 11.06 (s, NH, D_2O exchangeable), 12.24 (s, NH, D_2O exchangeable).

^{13}C NMR (DMSO-d_6, 100 MHz): 15.11, 21.63, 51.01, 115.45, 123.86, 124.56, 124.85, 125.82, 127.79, 129.02, 129.30, 133.69, 139.76, 141.51, 146.59, 148.29, 149.17, 151.47, 172.60 [*m*/*z* (rel. abundance)]: 429 (M^++1, 12%), 427 (M^+−1, 30%), 391 (25%), 298 (11%), 268 (56%), 252 (100%), 161 (39%). Anal. Calcd for $C_{23}H_{24}N_8O$ (FW: 428.21): C, 64.47; H, 5.65; N, 26.15. Found: C, 64.32; H, 5.81; N, 26.30.

4.1.12. 3-2-((5-(4-Acetylpiperazin-1-yl)-3-methyl-1-phenyl-1H-pyrazol-4-yl)methylene)hydrazinyl)quinoxalin-2(1H)-one (**15**)

R_f: 0.16 (Petroleum ether/Ethyl acetate, 0.5: 3), yield: 53.33%, m.p.: above 300. IR (KBr) (υ_{max}/cm^{-1}) 3425 (NH of quinoxaline), 3382 (NH hydrazinyl), 3055 (CH aromatic), 3000 (Intramolecular hydrogen bonded NH), 2926, 2847 (CH aliphatic), 1672 (C=O of quinoxalinone and acetyl), 1620 (C=N), 1560 (C=C aromatic). ^1H NMR(DMSO-d_6, 500 MHz): 2.46 (s, 3H, CH_3 of acetyl), 2.54 (s, 3H, CH_3), 2.76–2.84 (m, 4H, H2, H6 of piperazine protons), 2.95–3.14 (m, 4H, H3, H5 of piperazine protons), 7.04–7.13 (m, 3H, H3, H4, H5 of phenyl protons), 7.27–7.35 (m, 2H, H2, H6 of phenyl protons), 7.39–7.42 (m, 2H, quinoxaline protons), 7.57–7.62 (m, 2H, quinoxaline protons), 8.70 (s, 1H, CH=N), 11.04 (s, NH, D_2O exchangeable), 12.26 (s, NH, D_2O exchangeable). ^{13}C NMR (DMSO-d_6, 100 MHz): 15.11, 21.53, 108.81, 115.36,123.80, 124.76, 125.75, 127.80, 128.93, 133.61.61, 139.62, 141.42, 146.52, 148.21, 149.21, 151.39, 172.50 .

MS: [*m*/*z* (rel. abundance)]: 472 (M^++2, 19%), 469 (M^+−1, 14%), 399 (15%), 320 (32%), 298 (11%), 268 (56%), 251 (100%), 161 (39%). Anal. Calcd for $C_{25}H_{26}N_8O_2$ (FW: 470.22): C, 63.82; H, 5.57; N, 23.81. Found: C, 63.62; H, 5.69; N, 23.81.

4.1.13. 3-(2-((3-Methyl-1-phenyl-5-(4-(phenylsulfonyl)piperazin-1-yl)-1H-pyrazol-4-yl)methylene)hydrazinyl)quinoxalin-2(1H)-one (**16**)

R_f: 0.29 (Pet. ether/Ethyl acetate, 0.5: 3), yield: 66.66%, m.p: above 300. IR (KBr) (υ_{max}/cm^{-1}): 3421 (NH of quinoxaline), 3272 (NH hydrazinyl), 3044 (CH aromatic), 3000 (Intramolecular hydrogen bonded NH), 2896 (CH aliphatic), 1674 (C=O of quinoxalinone), 1613 (C=N), 1543 (C=C aromatic), 1447 ($\upsilon_{as}SO_2$), 1346 (υ_sSO_2). ^1H NMR(DMSO-d_6, 500 MHz): 2.41 (s, 3H, CH_3), 2.95–3.2 (m, 4H, H2, H6 of piperazine protons), 3.32–3.4 (m, 4H, H3, H5 of piperazine protons), 7.01–7.13 (m, 6H, H3, H4, H5 of phenyl protons and benzene sulfonyl protons), 7.27–7.3 (m, 2H, H2, H6 of benzene sulfonyl protons), 7.31–7,39 (m, 2H, H2, H6 of phenyl protons), 7.4–7.5 (m, 2H, quinoxaline protons), 7.58–7.7 (m, 2H, quinoxaline protons), 8.75 (s, 1H, CH=N), 11.04 (s, NH, D_2O exchangeable). 15.03, 108.81, 115.37, 123. 81, 125.22, 125.76, 127.72, 128.92, 129.23, 130.83, 132.69, 133.61, 135.58, 139.62, 141.43, 146.52, 148.21, 149.21, 151.40, 172.6. MS: [*m*/*z* (rel. abundance)]: 568 (M^+, 10%), 451 (35%), 438 (32%), 237 (21%), 211 (36%), 161 (100%). Anal. Calcd for $C_{29}H_{28}N_8O_3S$ (FW: 568.20): C, 61.25; H, 4.96; N, 19.71; S, 5.64. Found: C, 61.41; H, 4.79; N, 19.78; S, 5.51.

4.1.14. 3-(2-((3-Methyl-5-(4-(2-nitrophenylsulfonyl)piperazin-1-yl)-1-phenyl-1H-pyrazol-4-yl)methylene)hydrazinyl)quinoxalin-2(1H)-one (**17**)

R_f: 0.5 (Petroleum ether/Ethyl acetate, 0.5: 3), yield: 61.53%, m.p.: above 300 °C. IR (KBr) (υ_{max}/cm^{-1}): IR (KBr) (υ_{max}/cm^{-1}): 3425 (NH of quinoxaline), 3383 (NH hydrazinyl), 3000 (Intramolecular hydrogen bonded NH), 3032 (CH aromatic), 2939, 2848 (CH aliphatic), 1675 (C=O of quinoxalinone), 1613, (C=N), 1587 (C=O), 1547 (υ_{as} NO_2 & C=C aromatic), 1500 ($\upsilon_{as}SO_2$), 1438 (υ_sNO_2), 1355 (υ_sSO_2). ^1H NMR(DMSO-d_6, 500 MHz): 2.33 (s, 3H, CH_3), 3.04–3.18 (m, 4H, H2, H6 of piperazine protons), 3.2–3.33 (m, 4H, H3, H5 of piperazine protons), 7.05–7.16 (m, 5H, H2, H3, H4, H5, H6 of phenyl protons), 7.26–7.38 (m, 4H, quinoxaline protons), 7.39–7.45 (m, 2H, H4, H5 of nitrobenzenesulfonyl protons),

7.57–7.62 (m, 1H, H6 of nitrobenzenesulfonyl protons), 7.94–8 (m, 1H, H3 of nitrobenzenesulfonyl protons), 8.75 (s, 1H, CH=N), 11.04 (s, NH, D_2O exchangeable), 12.31 (s, NH, D_2O exchangeable). ^{13}C NMR (DMSO-d_6, 125 MHz): 15.05, 108.83, 115.36, 123.80, 124.50, 125.75, 127.71, 128.95, 133.63, 139.63, 141.42, 146.53, 148.20, 149.12, 151.40, 155.39, 172.2. MS: [*m*/*z* (rel. abundance)]: 613 (M^+, 10%), 615 (M^++2, 1.75%) 450 (30%), 161 (100%). Anal. Calcd for $C_{29}H_{27}N_9O_5S$ (FW: 613.65): C, 56.76; H, 4.43; N, 20.54; S, 5.23. Found: C, 56.00; H, 4.43; N, 19.95; S, 5.32.

4.1.15. General procedure for synthesis of compounds ***18–22***

A mixture of *N*-methyl piperazine, cyclopentanol, 2-mercaptoethanol, thioglycolic acid or dimethylamine (5.29 mmol) in 15 mL DMF and sodium hydride (10.58 mmol) was stirred for one hour, then a solution of compound **11a** (5.29 mmol) in dry DMF (10 mL) was added portion wise. The reaction mixture was refluxed for 8 h. After cooling the reaction was poured on iced water with stirring. Diluted HCl was used to allow the precipitation of the product at pH = 7. The precipitated product was filtered off and crystallized using ethanol.

*4.1.15.1. 3-(2-((3-Methyl-5-(4-methylpiperazin-1-yl)-1-phenyl-1H-pyrazol-4-yl)methylene)hydrazinyl)quinoxalin-2(1H)-one (**18**).* R_f: 0.23 (Ethyl acetate/petroleum ether/ethanol, 3:0.5:3 drops), Yield = 52.17%, m.p: 273–275 °C. IR(KBr) (υ_{max}/cm^{-1}): 3411 (NH of quinoxaline), 3059 (CH aromatic), 2920 (CH aliphatic), 1670 (C=O quinoxaline), 1615 (C=N). ^1H NMR (DMSO-d_6, 500 MHz): 2.32 (s, 3H, CH_3 of piperazine), 2.44 (s, 3H, CH_3), 2.76–2.79 (m, 4H, H2, H6, of piperazine protons), 2.82–2.91 (m, 4H, H3, H5 of piperazine protons), 7.11–7.22 (m, 3H, H3, H4, H5 of phenyl protons), 7.32–7.42 (m, 2H, H2, H6, of phenyl protons), 7.83 (s, 1H, CH=N) 7.97–8.2 (m, 4H, quinoxaline protons) 10. 45 (s, NH, D_2O exchangeable), 12.56 (br., NH, D_2O exchangeable). ^{13}C NMR (DMSO-d_6, 125 MHz): 15.41, 43.56, 46.21, 49.32, 114.32, 115.22, 123.11, 124.32, 125.74, 126.06, 127.90, 129.32, 133.29, 137.65, 139.72, 148.96, 151.21, 163.53. Mass Ms, *m*/*z* (%):442 (M^+, 1.1%), 186 (100%), 255 (0.75%), 158 (81.97%). Anal. Calcd for $C_{24}H_{26}N_8O$ (FW: 442.22): C, 65.14; H, 5.92; N, 25.32; Found: C, 64.55; H, 5.55; N, 25.49.

*4.1.15.2. 3-(2-((5-(Cyclopentyloxy)-3-methyl-1-phenyl-1H-pyrazol-4-yl)methylene)hydrazinyl)quinoxalin-2(1H)-one (**19**).* R_f: 0.21 (Ethyl acetate/petroleum ether/ethanol, 3:0.5: 3 drops), Yield: 60.7%, m.p.: 279–282 °C. IR (KBr) (υ_{max}/cm^{-1}): 3424 (NH of quinoxaline), 3000 (Intramolecular hydrogen bonded NH), 3060 (CH aromatic), 2952 (CH aliphatic), 1683 (C=O of quinoxaline), 1623 (CH=N), 1248 (ether linkage). ^1H NMR(DMSO-d_6, 500 MHz):1.8–1.92 (m, 2H, H2, H5, of cyclopentanol protons), 2.09–2.12 (m, 2H, H3, H4 of cyclopentanol protons), 2.36–2.40 (m, 1H of cyclopentanol protons), 2.49 (s, 3H, CH_3), 7.29–7.39 (3H, H3, H4, H5 of phenyl protons), 7.40–7.47 (m, 2H, H2, H6 of phenyl protons), 7.57–7.79 (m, 4H, quinoxaline protons), 8.43 (s, 1H, CH=N), 10.345 (s, NH, D_2O exchangeable), 12.5 (br., NH, D_2O exchangeable). ^{13}C NMR (DMSO-d_6, 125 MHz): 14.91, 29.18, 33.92, 98.2, 115.43, 117.34, 119.66, 120.76, 123.50, 124.22, 125.65, 126.98, 128.61, 129.11, 139.43, 142.84, 146.30, 148.26, 152.11, 158.99. Ms, *m*/*z* (%): 429 (M^++1, 0.27%), 185 (2.19%), 161 (2.67%), 63 (100%), Anal. Calcd for $C_{24}H_{24}N_6O_2$ (FW: 428.486): C, 67.27; H, 5.65; N, 19.61. Found: C, 67.55; H, 5.77; N, 19.7.

*4.1.15.3. 3-(2-((5-(2-Hydroxyethylthio)-3-methyl-1-phenyl-1H-pyrazol-4-yl)methylene)hydrazinyl)quinoxalin-2(1H)-one (**20**).* R_f: 0.25 (Ethyl acetate/petroleum ether/ethanol, 3:0.5:3 drops), Yield = 60.7%, m.p. = 279–283 °C. IR (KBr) (υ_{max}/cm^{-1}): 3397 (NH of quinoxaline), 3000 (Intramolecular hydrogen bonded NH), 3050 (CH aromatic), 2922 (CH aliphatic), 1666 (C=O of quinoxaline), 1617 (CH=N). ^1H NMR (DMSO-d_6,500 MHz): 2.36 (s, 2H, CH_2), 2.76 (s, 2H, CH_2), 2.47 (s, 3H, CH_3), 5.02 (s, 1H, OH, D_2O exchangeable), 7.20–7.28 (m, 2H, H2, H6 of phenyl protons), 7.41–7.54 (m,4H, H3, H4, H5 of phenyl protons, CH=N), 7.77–7.92 (m, 4H, quinoxaline protons), 10.62 (s, 1H, NH, D_2O exchangeable) 12.02 (s, 1H, NH, D_2O exchangeable). ^{13}C NMR (DMSO-d_6, 100 MHz): 14.47, 20.38, 59.90, 114.9, 115.04, 116.65, 118.98, 121.09, 122.90, 123.06, 125.54, 127.40, 129.21, 133.14, 143.09, 144.19, 151.73, 152.39, 155.04, 162.35. Ms, *m*/*z* (%): 420 (M^+, 34.47%), 422 (M^++2, 9.96%), 357 (100%), 185 (82.88%). Anal. Calcd for $C_{21}H_{20}N_6O_2S$ (FW: 420.48): C, 59.98; H, 4.79; N, 19.99; S, 7.61. Found: C, 59.82; H, 4.84; N, 19.76; S, 7.73.

*4.1.15.4. 2-(3-Methyl-4-((2-(3-oxo-3,4-dihydroquinoxalin-2-yl) hydrazono)methyl)-1-phenyl-1H-pyrazol-5-ylthio)acetic acid (**21**).* R_f: 0.3 (Ethyl acetate/petroleum ether/ethanol, 3:0.5: 3 drops), Yield: 60.7%, m.p.: 289–292 °C IR (KBr) (υ_{max}/cm^{-1}): 3379 (NH of quinoxaline), 3061 (CH aromatic), 2921 (CH aliphatic), 1687 (C=O of quinoxaline), 1617 (CH=N). ^1H NMR (DMSO-d_6,500 MHz): 2.42 (s, 3H, CH_3), 4.21 (s, 2H, CH_2), 7.19–7.42 (m, 5H, H2, H3, H4, H5, H6 of phenyl protons), 7.52–7.89 (m, 4H, quinoxaline protons), 7.92 (s, 1H, CH=N), 9.16 (s, 1H, NH, D_2O exchangeable), 12.09 (s, 1H, OH group), 13.76 (br., 1H, OH, COOH). ^{13}C NMR (DMSO-d_6, 125 MHz): 15.21, 48.33, 114.76, 115.59, 117.31, 120.25, 121.02, 122.42, 123.47, 123.99, 125.14, 126.26, 127.82, 128.42, 129.37, 139.24, 140.10, 140.43, 141.49, 143.14, 150.47, 150.50, 150.79, 152.24, 155.25, 164.32, 170.12. Ms, *m*/*z* (%): 436 (M^++2, 0.8%), 434 (M^+, 1.27%), 18 (100%). Anal. Calcd for $C_{21}H_{18}N_6O_3$ (FW: 434.47): C, 58.05; H, 4.18; N, 19.34; S, 7.38. Found: C, 58.25; H, 4.31; N, 19.5; S, 7.28.

*4.1.15.5. 3-(2-((5-(Dimethylamino)-3-methyl-1-phenyl-1H-pyrazol-4-yl)methylene)hydrazinyl)quinoxalin-2(1H)-one (**22**).* R_f: 0.21 (Ethyl acetate/petroleum ether/ethanol, 3:0.5: 3 drops), Yield: 60.7%, m.p.: above 300 °C. IR (KBr) (υ_{max}/cm^{-1}): 3435 (NH of quinoxaline), 3137 (NH, hydrazinyl quinoxaline), 3049 (CH aromatic), 2916, 2871 (CH aliphatic), 1682 (C=O of quinoxaline), 1588 (C=N). ^1H NMR (DMSO-d_6,500 MHz): 2.14 (s, 3H, CH3), 2.16 (s, 3H, CH_3), 2.49 (s, 3H, CH3), 7.13–7.24 (m, 3H, H3, H4, H5 of phenyl protons), 7.34–7.44 (m, 2H, H2, H6 of phenyl protons), 7.62–7.7 4 (m, 2H, quinoxaline protons), 7.81–7.92 (m, 2H, quinoxaline protons), 8.98 (s, 1H, CH=N), 12.23 (br., OH and NH D_2O exchangeable). ^{13}C NMR (DMSO-d_6, 125 MHz): 13.15, 40.39, 40.6, 116.34, 117.11, 121.76, 123.43, 125.79, 127.23, 128.61, 129.59, 129.86, 130.51, 137.09, 142.00, 145.51, 149.87, 152.29, 159.38. Ms, *m*/*z* (%): 388 (M^++1, 0.68%), 387 (M^+, 0.23%), 258 (65.45%), 161 (21.05%), 63 (100%). Anal. Calcd for $C_{21}H_{21}N_7O$ (FW: 387.18), C, 65.10; H, 5.46; N, 25.31. Found: C, 65.00; H, 5.33; N, 25.24.

4.2. Cytotoxic activity

Cells were plated in 96-multiwell plate (10^4 cells/well) for 24 h before treatment with the compounds to allow attachment of the cells to the wall of the plate. Different concentrations of the compounds under test (0, 12.5, 25, 50 μg/mL) were added to the cell monolayer. Triplicate wells were prepared for each individual dose. Monolayer cells were incubated with the compounds for 48 h at 37 °C and in atmosphere of 5% CO_2. After 48 h, cells were fixed, washed and stained with (Sulforhodamine B) stain. Excess stain was washed with acetic acid and attached stain was recovered with Tris EDTA buffer. Color intensity was measured in an ELISA reader. The relation between surviving fraction and drug concentration is plotted to get the survival curve of each tumor cell line after the specified compound was added. IC_{50} values of the tested compounds were calculated by Graph Pad Prism 5 software [32].

4.3. Protein kinase inhibition

The effect of tested compounds on the level of human tyrosine kinase (TRK) were determined utilizing 2 different human tumor cell lines including breast cancer cell line MCF-7 and liver cancer cell line HepG2 were obtained from the American Type Culture Collection (Rockville, MD, USA). The tumor cells were maintained in Dulbecco's modified Eagle's medium (DMEM) supplemented with 10% heat inactivated fetal calf serum (GIBCO), penicillin (100 U/mL) and streptomycin (100 μg/mL) at 37 °C in humidified atmosphere containing 5% CO_2. Cells at a concentration of 0.50×10^6 were grown in a 25 cm^2 flask in 5 mL of complete culture medium.

The cells in culture medium were treated with 20 μL of IC_{50} values of the compounds or the standard reference drug, cisplatin dissolved in DMSO, then incubated for 24 h at 37 °C, in a humidified 5% CO_2 atmosphere. The cells were harvested and homogenates were prepared in saline using a tight pestle homogenizer until complete cell disruption.

A double-antibody sandwich enzyme-linked immunosorbent assay (ELISA) of human tyrosine kinase kit purchase from Glory Science Co., Ltd (Del Rio, TX 78840, USA) was used to determine the level of TRK in the samples according to the manufacturer's instructions. This assay is based on that, add TRK to monoclonal antibody enzyme well which is pre-coated with human TRK monoclonal antibody, incubation; then, add TRK antibodies labeled with biotin, and combined with Streptavidin-HRP to form immune complex; then carry out incubation and washing again to remove the uncombined enzyme. Then add Chromogen solution A, B, the color of the liquid changes into the blue, and at the effect of acid, the color finally becomes yellow. The chroma of color and the concentration of the human TRK of sample were positively correlated and the optical density was determined at 450 nm. The level of TRK in samples was calculated as triplicate determinations from the standard curve and the percentage of TRK inhibition for each compound was calculated as compared with control cancer cells (DMSO treated).

4.4. Molecular docking study

The studied inhibitors were built using MOE (Chemical Computing Group, Montreal, CA). The crystal structure of c-kit in complex with STI-571 (Imatinib or Gleevec) was retrieved from the Protein Data Bank (PDB code: 1T46). The protein was prepared (hydrogen atoms addition, water removed and ligand extracted) with GOLD [26], V 5.1 (CCDC, Cambridge, UK) using default parameters. The docking program GOLD was used to operate the docking of compounds **11a**, **11b**, **12**, **13**, **14**, **15**, **16**, **17**, **18**, **20**, **21** and **22** into the crystal structure of c-kit. The active site was defined specifying all residues around the co-crystallized ligand in a sphere of 7 Å radius. All docking runs were performed three times using standard default variables. In some branched compounds (**12**, **13**, **14**, and **15**) the docking was constrained to force a hydrogen bonds with GLU640 and ASP810 to generate similar poses as the parent drug **11a** and **11b** and comparable to the previous publication. The docking protocol utilized the analysis of top ten docked solutions per ligand. The software Ligandscout was used to generate a 3D pharmacophore from the ligand of the PDB structure 1T46 with default parameters. This pharmacophore was used to prioritize the superior docking poses of the studied compounds. The most plausible conformation was selected for each ligand based on its ability to achieve the highest amount of chemical interactions described in the 3D pharmacophore.

4.5. In vitro cyclooxygenase (COX) inhibition assay

The ability of the test compounds to inhibit ovine COX-1 and COX-2 was determined using an enzyme immunoassay (EIA) (kit catalog number 560131, Cayman Chemical, Ann Arbor, MI, USA) according to the manufacturer's instructions. Cyclooxygenase catalyzes the first step in the biosynthesis of arachidonic acid (AA) to PGH_2. $PGF_{2\alpha}$, produced from PGH_2 by reduction with stannous chloride, is measured by enzyme immunoassay (ACE™ competitive EIA). Stock solutions of test compounds were dissolved in a minimum volume of DMSO. Briefly, to a series of supplied reaction buffer solutions (960 μL, 0.1 M Tris–HCl pH 8.0 containing 5 mM EDTA and 2 mM phenol) with either COX-1 or COX-2 (10 μL) enzyme in the presence of heme (10 μL) were added 10 μL of various concentrations of test drug solutions (0, 0.01, 0.1, 1, 10 and 50 μM in a final volume of 1 mL). These solutions were incubated for a period of 5 min at 37 °C after which 10 μL of AA (100 μM) solution were added and the COX reaction was stopped by the addition of 50 μL of 1 M HCl after 2 min. $PGF_{2\alpha}$, produced from PGH_2 by reduction with stannous chloride was measured by enzyme immunoassay. This assay is based on the competition between PGs and a PG-acetylcholinesterase conjugate (PG tracer) for a limited amount of PG antiserum. The amount of PG tracer, that is, able to bind to the PG antiserum is inversely proportional to the concentration of PGs in the wells since the concentration of PG tracer is held constant while the concentration of PGs varies. This antibody–PG complex binds to a mouse anti-rabbit monoclonal antibody that had been previously attached to the well. The plate is washed to remove any unbound reagents and then Ellman's reagent, which contains the substrate to acetylcholine esterase, is added to the well. The product of this enzymatic reaction produces a distinct yellow color that absorbs at 410 nm. The intensity of this color, determined spectrophotometrically, is proportional to the amount of PG tracer bound to the well, which is inversely proportional to the amount of PGs present in the well during the incubation: Absorbance α [Bound PG Tracer] $\alpha 1$/PGs. Percent inhibition was calculated by the comparison of compound treated to various control incubations. The concentration of the test compound causing 50% inhibition (IC_{50}, μM) was calculated from the concentration–inhibition response curve (duplicate determinations).

Acknowledgment

We thank the National Research Centre, Cairo, Egypt and the Science and Technological Development Fund (STDF), Egypt, for supporting the present manuscript through the STDF grant ID 1517.

Appendix A. Supplementary data

Supplementary data related to this article can be found at http://dx.doi.org/10.1016/j.ejmech.2014.08.048.

References

[1] S.T. Al-Rashood, I.A. Aboldahab, M.N. Nagi, L.A. Abouzeid, A.A.M. Abdel-Aziz, S.G. Abdel-Hamide, K.M. Youssef, A.M. Al-obaid, H.I. El-Subbagh, Bioorg. Med. Chem. 14 (2006) 8608–8621.
[2] A.M. Al-obaid, S.G. Abdel-Hamid, H.A. El-Kashef, A.A.M. Abdel-Aziz, A.S. El-Azab, H.A. Al-khamees, H.I. EL-Subbagh, Eur. J. Med. Chem. 44 (2009) 2379–2391.
[3] F.A.M. Al-Omary, L.A. Abouzeid, M.N. Nagi, E.E. Habib, A.A.M. Abdel-Aziz, A.S. El-Azab, S.G. Abdel-Hamide, M.A. Al-Omar, A.M. Al-obaid, H.I. El-Subbagh, Bioorg. Med. Chem. 18 (2010) 2849–2863.
[4] H. Gao, E.F. Yamasaki, K.K. Chan, L.L. Shen, R.M. Snapka, Mol. Pharmacol. 63 (2003) 1382–1388.
[5] H. Gao, K.-C. Huang, E.F. Yamasaki, K.K. Chan, L. Chohan, R.M. Snapka, PNAS 96 (1999) 12168–12173.
[6] J.J. Reiners, M. Kleinman, A. Joiakim, P.A. Mathieu, J. Pharmacol. Exp. Ther. 328 (2009) 796–806.
[7] E.J. Mensah-Osman, A.M. Al-Katib, M.H. Dandashi, R.M. Mohammad, Mol. Cancer Ther. 14 (2002) 1315–1320.
[8] E.J. Mensah-Osman, A.M. Al-Katib, M.H. Dandashi, R.M. Mohammad, Mol. Cancer Ther. 14 (2002) 1321–1326.

[9] T. S Bekaii-Saab, A. Mortazavi, L.G. Hicks, M. Zalupski, R.J. Pelley, K.K. Chan, E.H. Kraut, Invest. New. Drugs 24 (2006) 343–346.
[10] H. Gao, E.F. Yamasaki, K.K. Chan, L.L. Shen, R.M. Snapka, Cancer Res. 60 (2000) 5937–5940.
[11] I. Shchemelinin, L. Šefc, E. Nečas, Folia Biol. (Praha) 52 (2006) 81–101.
[12] J.A. Adams, Chem. Rev. 101 (2001) 2271–2290.
[13] Y. Yarden, M.X. Sliwkowski, Natl. Rev. 2 (2001) 127–137.
[14] J. Dumas, C. Opin, Drug Discov. Dev. 4 (2001) 378–381.
[15] M. Kovalenko, A. Gazit, A. Bohmer, C. Rorsman, L. Ronnstrand, C. Heldin, J. Waltenberger, F.D. Bohmer, A. Levitzki, Cancer Res. 54 (1994) 6106–6114.
[16] M.A. Bogoyevitch, R.K. Barr, A.J. Ketterman, Biochim. Biophys. Acta 1754 (2005) 79–99.
[17] S.A. Galal, A.S. Abdelsamie, H. Tokuda, N. Suzuki, A. Lida, M.M. ElHefnawi, R.A. Ramadan, M.H.E. Atta, H.I. El Diwani, Eur. J. Med. Chem. 46 (2011) 327–340.
[18] R.M. Claramunt, L. Bouissane, M.P. Cabildo, M.P. Cornago, J. Elguero, A. Radziwon, C. Medina, Bio. Med. Chem. 17 (2009) 1290–1296.
[19] T.D. Penning, J.J. Talley, S.R. Bertenshaw, J.S. Carter, P.W. Collins, S. Docter, M.J. Graneto, L.F. Lee, J.W. Malecha, J.M. Miyashiro, R.S. Rogers, D.J. Rogier, S.S. Yu, G.D. Anderson, E.G. Burton, J.N. Cogburn, S.A. Gregory, C.M. Koboldt, W.E. Perkins, K. Seibert, A.W. Veenhuizen, Y.Y. Zhang, P.C. Isakson, J. Med. Chem. 40 (1997) 1347–1365.
[20] Q.P. Peterson, D.C. Hsu, D.R. Goode, C.J. Novotny, R.K. Totten, P. Hergenrother, J. Med. Chem. 52 (2009) 5721–5731.
[21] J. Regan, S. Breitfelder, P. Cirillo, T. Gilmore, A.G. Graham, E. Hickey, B. Klaus, J. Madwed, M. Moriak, N. Moss, C. Pargellis, S. Pav, A. Proto, A. Swinamer, L. Tang, C. Torcellini, J. Med. Chem. 45 (2002) 2994–3000.
[22] R. Aggarwal, A. Bansal, I. Rozas, B. Kelly, P. Kaushik, D. Kaushik, Eur. J. Med. Chem. 70 (2013) 350–457.
[23] S.M. Sakya, K.M. DeMello, M.L. Minich, B. Rast, A. Shavnya, R.J. Rafka, D.A. Koss, H. Cheng, J. Li, B.H. Jaynes, C.B. Ziegler, D.W. Mann, C.F. Petras, S.B. Seibel, A.M. Silvia, D.M. George, L.A. Lund, S.S. Denis, A. Hickman, M.L. Haven, M.P. Lynch, Bio. Med. Chem. Lett. 16 (2006) 288–292.
[24] S.M. Sakya, H. Cheng, K.M. DeMello, A. Shavnya, M.L. Minich, B. Rast, J. Dutra, C. Li, R.J. Rafka, D.A. Koss, J. Li, B.H. Jaynes, C.B. Ziegler, D.W. Mann, C.F. Petras, S.B. Seibel, A.M. Silvia, D.M. George, A. Hickman, M.L. Haven, M.P. Lynch, Bio. Med. Chem. Lett. 16 (2006) 1202–1206.
[25] K.M. Leahy, R.L. Ornberg, Y. Wang, B.S. Zweifel, A.T. Koki, J.L. Masferrer, Cancer Res. 62 (2002) 625–627.
[26] Z.J. Zhou, S. Yan, L. Ma, Bioorg. Med. Chem. 21 (2013) 2156–2162.
[27] B.P. Bandgar, J.V. Totre, S.S. Gawande, C.N. Khobragade, S.C. Warangkar, P.D. Kadam, Bioorg. Med. Chem. 18 (2010) 6149–6155.
[28] A.M. Mohamed, W.A. El-Sayed, M.A. Alsharari, H.R. Al-Qalawi, M.O. Gemoush, Arch. Pharm. Res. 36 (2013) 1055–1065.
[29] I. Koca, A. Özgür, K.A. Coşkun, Y. Tutar, Bioorg. Med. Chem. 21 (2013) 3859–3865.
[30] E.A. Dikusar, V.I. Potkin, N.G. Kozlov, Russ. J. Gen. Chem. 78 (2008) 1569–1572.
[31] M.-S. Park, H.-J. Park, H. Koon, K.-I. Lee, Synth. Commun. 34 (2004) 1541–1550.
[32] P. Skehan, R. Storeng, D. Scudiero, A. Monks, J. McMahon, D. Vistica, J.T. Warren, H. Bokesh, S. Kenney, M.R. Boyd, J. Natl. Cancer Inst. 82 (1990) 1107–1112.
[33] C.E. Edling, B. Hallberg, Int. J. Biochem. Cell Biol. 39 (2007) 1995–1998.
[34] S.A. Galal, A.S. Abdelsamie, S.M. Solima, J. Mortier, G. Wolber, M.M. Ali, H. Tokuda, N. Suzuki, A. Lida, R.A. Ramadan, M.H.E. Atta, H.I. El Diwani, Eur. J. Med. Chem. 69 (2013) 115–124.
[35] G. Wolber, A. Dornhofer, T. Langer, J. Chem. Inf. Model. 45 (2005) 160–169.
[36] C.D. Mol, D.R. Dougan, T.R. Schneider, R.J. Skene, M.L. Kraus, D.N. Scheibe, G.P. Snell, H. Zou, B.C. Sang, K.P. Wilson, J. Biol. Chem. 30 (2004) 31655–31663.
[37] G. Jones, P. Willett, R.C. Glen, A.R. Leach, R. Taylor, J. Mol. Biol. 267 (1997) 727–748.
[38] M. Macarthur, G.L. Hold, E.M. El-Omar, J. Phys. Gastrointest. Liver Physiol. 286 (2004) 515–520.